# Separation of Fullerenes $C_{60}$ and $C_{70}$ Using a Crystallization-Based Process

**Kui S. Kwok, Yik C. Chan, and Ka M. Ng**
Dept. of Chemical and Biomolecular Engineering, The Hong Kong University of Science and Technology, Clear Water Bay, Hong Kong

**Christianto Wibowo**
ClearWaterBay Technology Inc., 4000 W. Valley Boulevard, Suite 100, Pomona, CA 91789

*DOI 10.1002/aic.12105*
*Published online November 9, 2009 in Wiley InterScience (www.interscience.wiley.com).*

*A crystallization-based process that separates pure fullerenes $C_{60}$ and $C_{70}$ from their mixture using o-xylene as the solvent has been developed. Isothermal solid–liquid equilibrium phase diagrams of the $C_{60}$-$C_{70}$-o-xylene ternary system for a number of temperatures were first determined at 1 atm. Taking advantage of the shift in solvent-free composition of the $C_{60}$-$C_{70}$ double saturation point with temperature and based on the solid solution-forming phase behavior between $C_{60}$ and $C_{70}$, the flowsheet of a general crystallization process was then synthesized. It involved the fractionation of a $C_{60}$-$C_{70}$ fullerene mixture into $C_{60}$-rich and $C_{70}$-rich solid solutions using temperature-swing crystallization, followed by purification of the solid solutions with multistage crystallization into pure $C_{60}$ and $C_{70}$ solids. To demonstrate process feasibility, bench-scale batch experiments were performed using a commercially available fullerene mixture that was pretreated by adsorption to remove higher fullerenes. $C_{60}$ and $C_{70}$ solids of purity higher than 99 wt % were obtained.* © 2009 American Institute of Chemical Engineers *AIChE J,* 56: 1801–1812, 2010

*Keywords: fullerenes, crystallization, process synthesis, solid–liquid equilibrium phase diagram, solid solution*

## Introduction

The unique structures and interesting properties exhibited by fullerenes have inspired scientists to conduct research on the potential applications of this carbon allotrope in a wide variety of fields. For example, the high electron affinity and the ability to transport charge effectively render pure $C_{60}$ and $C_{70}$, the two most abundant fullerene species, the best available electron acceptors in organic solar cells and photovoltaic devices to date.[1–4] Being efficient radical scavengers, or generators of reactive oxygen species upon photosensitization, $C_{60}$ and their derivatives are also found to be useful in a number of biological or medicinal areas, including drug delivery,[5] neuroprotection and antioxidation,[6] antiviral activity,[7] antibacterial action,[8] cancer/tumor therapy,[9] and imaging and contrast agents.[10] In addition, the fact that $C_{60}$ and $C_{70}$ can absorb more laser radiation in excited states than in their ground states leads to their possible utilization as optical limiters.[11] Exploitation of pure fullerenes in other subjects, such as sensors, catalysts, superconductors, and fuel cells, is also under investigation.

Despite the progress in exploring the applications of fullerenes, further development and commercialization of fullerene-based products are hampered by the limited availability and high cost of pure fullerenes. The cause of difficulty lies in the separation of mixed fullerenes. The existing synthesis methods of pure fullerenes usually include three steps. First, carbon soot that contains a mixture of fullerene species is produced using techniques such as vaporization of graphite by electric arc[12,13] or combustion of hydrocarbons in sooting

Correspondence concerning this article should be addressed to K. M. Ng at kekmng@ust.hk.

flames.[14,15] The fullerene-containing soot is then stirred in an organic solvent (e.g., toluene) in the second step to extract the soluble fullerenes. After filtering out the insoluble materials, fullerenes in the filtrate are separated to yield pure fullerenes. It is the lack of an effective and economical technique in this final step that sharply increases the price of pure fullerenes. Liquid chromatography,[16,17] the most widely used means for fullerene isolation and purification, suffers from the drawbacks of low product throughput and high capital cost related to the need for a large amount of stationary and mobile phases. Loss of fullerenes may also occur as some of them adsorb irreversibly on the stationary phase or decompose during processing.[16,18] In selective complexation,[19,20] which achieves the separation via host-guest interactions and preferential precipitation, rather complicated reaction and decomplexation steps are required. As a consequence, although mixed fullerenes (composed of, for instance, about 60 wt % $C_{60}$, 25 wt % $C_{70}$, and 15 wt % of other higher fullerenes up to $C_{96}$) can be purchased in kilogram or even ton quantities at around 4 US dollars per gram,[21] fullerenes of high purity are often supplied in gram or milligram level and at much higher prices. For example, 99% pure $C_{60}$ solids cost 40–45 US dollars per gram. The price of 99% pure $C_{70}$ solids is even higher, ranging from 450 to 500 US dollars per gram.

Continuing effort has, therefore, been made to search for more cost-effective separation alternatives. Crystallization, because of its relatively simple operation and its potential of being performed in large scale, is an attractive and promising option. However, only a very limited number of investigations, which use crystallization to separate mixed fullerenes primarily based on experimental trial-and-error, have been reported.[22–25] In the absence of a fundamental understanding of the process, a low-cost crystallization-based process has been out of reach.

A practical means to address this problem is to use phase diagram-guided process synthesis. The key idea of this approach is to determine and represent the solid–liquid phase equilibrium data of the system under consideration on a phase diagram. This allows the user to easily identify the thermodynamic features such as eutectic troughs, solubility surfaces, and crystallization region(s)/compartment(s) of the component(s) to be separated from the system. Based on the insights derived from visualization, a series of operations (such as heating, cooling, solvent addition/removal, and streams combination/split) can then be devised, which forms the basis for generating a crystallization-based process flowsheet. Details on the determination, representation, visualization, and utilization of phase diagrams for the synthesis of crystallization-based processes are available.[26–32]

The objective of this article is to demonstrate the application of phase diagram-aided synthesis for developing a novel crystallization-based separation scheme that produces both pure $C_{60}$ and $C_{70}$ solids from their mixture. The practicability of such a process will be validated with batch experiments using a commercially available fullerene mixture as the feed material and *o*-xylene as the solvent. *o*-Xylene is selected because it is the most suitable solvent in terms of its solubility for fullerenes, availability, cost, boiling point, and toxicity. Up to now, crystallization has been used primarily for recovering a relatively pure component from a liquid solution in solid form in industry. This technique is expected to be applicable for separating two-component and, with process modification, even multicomponent mixtures in a solvent other than the $C_{60}$ and $C_{70}$ mixture under consideration.

## Experimental Determination of the SLE Phase Diagram of Ternary System $C_{60}$-$C_{70}$-*o*-Xylene

It has been reported in the literature that within the temperature range of −20 to 80°C, the solubility of $C_{60}$ in *o*-xylene reaches a maximum at around 30°C, and beyond this point, the solubility drops with further increase in temperature. In contrast, the solubility of $C_{70}$ in *o*-xylene increases monotonically with temperature in the same temperature range.[33] Such a difference between the temperature dependence of the solubility of $C_{60}$ and $C_{70}$ offers a clue for separating pure $C_{60}$ and $C_{70}$ solids from their mixture by temperature-swing crystallization. To pursue this possibility, isothermal cuts of the phase diagram for the system $C_{60}$-$C_{70}$-*o*-xylene at different temperatures were generated.

### *Materials*

Fullerene $C_{60}$ (Nanom purple, purity >99%) and $C_{70}$ (purity >98%) solids used for solubility measurement were purchased from Frontier Carbon Corporation (FCC) and Nano-C, respectively. The solvent, *o*-xylene (purity ≥99.0%), was obtained from Fluka. All these materials were used without further purification.

### *Experimental setup and procedure*

The "analytical method" was used to determine the required isothermal phase diagrams, and the experimental setup used for measuring solubility is displayed in Figure 1. It consisted of four jacketed glass vessels that were connected in series via Tygon tubings to a water bath (Julabo, model F12 MB), which was used to control the temperature of the samples to within ±0.1°C of the desired value. To confirm that such a value was attained, the actual sample temperature was monitored by a Digi-Sense J-T-E-K thermocouple thermometer with a precision of 0.1°C. Mixing was provided to each of the four samples independently using a 4-in-1 hot plate magnetic stirrer (Cole Parmer).

In an experimental run, a solid mixture of desired composition was first prepared by weighing appropriate amounts of fullerene $C_{60}$ and $C_{70}$ into each of the four jacketed glass vessels. The total solid mass of a typical sample was about 0.1 g. Around 1.3 mL of *o*-xylene was then added to the solid mixture such that the solids were in excess. After inserting a magnetic stir bar, each vessel was closed with a stopper and further sealed with a strip of paraffin film or PTFE threadseal tape to avoid the loss of solvent due to evaporation. Next, the four vessels were connected to the water bath and the samples were stirred at the predetermined temperature for 24 h. This duration had been confirmed by preliminary tests to be sufficient for the samples to reach equilibrium. To prevent any degradation or photo-induced reaction of the fullerene samples caused by prolonged exposure to light, the vessels were covered with an aluminum foil throughout the entire experiment.

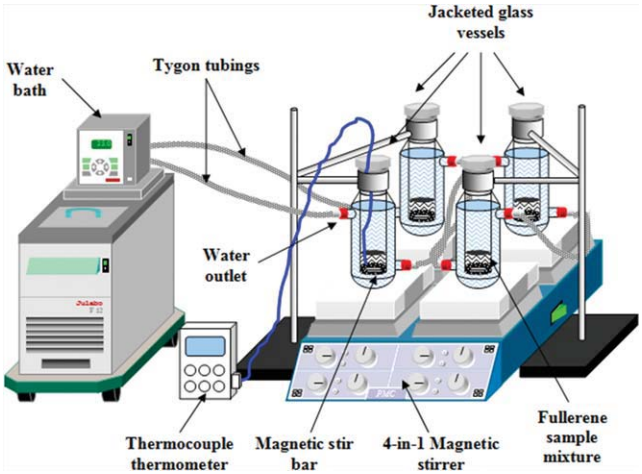


**Figure 1. Experimental setup for measuring solubility by analytical method.**

[Color figure can be viewed in the online issue, which is available at www.interscience.wiley.com.]

To extract the solid phase and the saturated liquid phase of an equilibrated sample, part of the solid–liquid mixture was quickly withdrawn from the vessel into a 1-mL disposable syringe, the temperature of which had to be brought to nearly the same value as that of the sample in advance. After installing a membrane filter (Advantec MFS, 13 mm dia., PTFE membrane, pore size 0.2 $\mu$m) to the syringe, the mixture was injected into a glass vial. In the course of such an injection, the liquid phase got into the vial while the solid particles were trapped inside the filter. The former was immediately diluted 100 times with toluene (HPLC grade, purity $\geq$99.7%, Mallinckrodt Chemicals) to make up a solution for composition analysis. For the solids caught in the syringe filter, they were first washed by 3 mL of *n*-hexane (HPLC grade, purity $\geq$95%, Fisher Chemicals) and then removed from the filter by dissolving in about 12 mL toluene to form another solution for subsequent analyses. The concentrations of fullerenes $C_{60}$ and $C_{70}$ in both types of solutions were determined using high-performance liquid chromatography (Waters Alliance HPLC system with a Waters 2695 Separations Module and a Waters 2996 Photodiode Array Detector). Carried by a mobile phase of 60% isopropyl alcohol (HPLC grade, purity $\geq$99.5%, Mallinckrodt Chemicals) and 40% toluene, the sample solutions were pumped through a C18 column (YMC-Pack, ODS(Octa-Deca-Silica)-A, pore size 12 nm, particle size 5 $\mu$m, 150 mm $\times$ 4.6 mm I.D.) operated at room temperature. The concentrations of $C_{60}$ and $C_{70}$ were detected at the wavelength of 330 and 308 nm, respectively.

### *Experimental results and discussion*

Solubility measurements were performed to determine the isothermal phase diagrams of the system $C_{60}$-$C_{70}$-*o*-xylene at 10, 30, and 60°C under atmospheric pressure. The results are summarized in Table 1, and the three isothermal cuts are plotted in Figures 2a–c, respectively. Because of the very low solubility of $C_{60}$ and $C_{70}$ in *o*-xylene at the temperature range studied (<0.05 in mass fraction), to facilitate data visualization, the triangular phase diagrams are presented in such a way that the region near the pure *o*-xylene vertex is enlarged, and the middle section of the diagram with mass fraction of *o*-xylene from 0.5 to 0.9 is omitted. The compositions of the solid and liquid phases from the same sample mixture are connected by a tie line (dotted/dashed line). It should also be noted that no analysis was conducted to check the presence of solvates in the solid phases, as the solid-phase extraction method described earlier only allowed the recovery of a solution of the solid phase in toluene rather than the solid phase itself. Thus, the solid phase compositions given in Table 1 are on a solvent-free basis, and all the data points for solid phases plotted in Figures 2a–c lie on the edge of zero mass fraction of *o*-xylene.

Four distinct features on the phase diagram of the ternary system $C_{60}$-$C_{70}$-*o*-xylene can be observed. First, fullerenes $C_{60}$ and $C_{70}$ form solid solutions with the presence of an immiscibility gap in the temperature range studied. Three different saturation regions can be identified on each of the isobaric–isothermal phase diagrams—a single saturation region for $C_{60}$-rich solid solution, a single saturation region for $C_{70}$-rich solid solution, and a double saturation region for $C_{60}$-rich and $C_{70}$-rich solid solutions (Figure 2, Table 2). Similar observations were reported by other researchers for the same system but at other temperatures.[34,35] Second, by comparing the solvent-free compositions of the initial sample mixtures with that of the resulting liquid and solid phases (Table 2), it can be found that the orientation of the tie lines in the single saturation region of $C_{60}$-rich solid solution favors the formation of a $C_{60}$-enriched solid solution, whereas that in the single saturation region of $C_{70}$-rich solid solution favors the formation of a $C_{70}$-enriched solid solution upon phase split. Thus, multistage crystallization can help to purify $C_{60}$ or $C_{70}$ solids once the composition of a mixture is directed into the corresponding single saturation region. The remaining problem is to bypass the double saturation point by moving the mixture composition from one single saturation region to another.

This challenge can be met because of the third feature shown in Figure 3. It provides a comparison of the solid–liquid saturation curves of the system at 10, 30, and 60°C, which are formed by manually joining the composition points of all the liquid phases presented in Figures 2a–c, respectively. There is a shift in the solvent-free composition of the double saturation point as the temperature is changed from 10 to 60°C. This shift is the key in using temperature swing plus solvent addition/removal to move back and forth the mixture composition between two single saturation regions.[29,32] Finally, the fourth feature in Figure 3 provides hints on how to execute the separation of the $C_{60}$-rich and $C_{70}$-rich solid solutions. The single saturation curve for $C_{60}$-rich solid solution moves away from the vertex of pure *o*-xylene from 10 to 30°C but moves toward it when temperature is further increased from 30 to 60°C. This means that the solubility of $C_{60}$-rich solid solution in *o*-xylene shows a maximum within the range of 10–60°C, and beyond the maximum point, the solubility decreases with temperature. In contrast, as the single saturation curve for $C_{70}$-rich solid solution moves farther and farther away from the pure *o*-xylene vertex when temperature is increased, $C_{70}$-rich solid solution shows a monotonically increasing solubility in *o*-xylene. Based on this feature, it can be concluded that a

**Table 1. Experimental Solid–Liquid Equilibrium Data for the Ternary System $C_{60}$-$C_{70}$-*o*-Xylene at 10, 30, and 60°C under Atmospheric Pressure**

| | | Composition of Initial Mixture (Mass Fraction) | | | Liquid-Phase Composition (Mass Fraction) | | | Solid-Phase Composition (Relative Mass Fraction Between $C_{60}$ and $C_{70}$) | |
|---|---|---|---|---|---|---|---|---|---|
| Temp. (°C) | Sample No. | $C_{60}$ | $C_{70}$ | *o*-Xylene | $C_{60}$ | $C_{70}$ | *o*-Xylene | $C_{60}$ | $C_{70}$ |
| 10 | 1 | 0.0263 | 0.0000 | 0.9737 | 0.0077 | 0.0000 | 0.9923 | 1.0000 | 0.0000 |
| | 2 | 0.0351 | 0.0028 | 0.9621 | 0.0081 | 0.0027 | 0.9892 | 0.9828 | 0.0172 |
| | 3 | 0.0316 | 0.0068 | 0.9616 | 0.0079 | 0.0069 | 0.9852 | 0.9763 | 0.0237 |
| | 4 | 0.0275 | 0.0103 | 0.9622 | 0.0084 | 0.0106 | 0.9809 | 0.9699 | 0.0301 |
| | 5 | 0.0239 | 0.0144 | 0.9617 | 0.0086 | 0.0136 | 0.9778 | 0.9093 | 0.0907 |
| | 6 | 0.0236 | 0.0186 | 0.9578 | 0.0089 | 0.0130 | 0.9781 | 0.7239 | 0.2761 |
| | 7 | 0.0203 | 0.0175 | 0.9622 | 0.0093 | 0.0130 | 0.9776 | 0.7121 | 0.2879 |
| | 8 | 0.0193 | 0.0231 | 0.9576 | 0.0094 | 0.0142 | 0.9764 | 0.5504 | 0.4496 |
| | 9 | 0.0168 | 0.0263 | 0.9569 | 0.0093 | 0.0142 | 0.9766 | 0.4420 | 0.5580 |
| | 10 | 0.0094 | 0.0239 | 0.9667 | 0.0092 | 0.0131 | 0.9777 | 0.0561 | 0.9439 |
| | 11 | 0.0067 | 0.0269 | 0.9664 | 0.0064 | 0.0130 | 0.9806 | 0.0421 | 0.9579 |
| | 12 | 0.0030 | 0.0298 | 0.9672 | 0.0031 | 0.0131 | 0.9839 | 0.0272 | 0.9728 |
| | 13 | 0.0000 | 0.0284 | 0.9716 | 0.0000 | 0.0130 | 0.9870 | 0.0000 | 1.0000 |
| 30 | 14 | 0.0443 | 0.0000 | 0.9557 | 0.0112 | 0.0000 | 0.9888 | 1.0000 | 0.0000 |
| | 15 | 0.0427 | 0.0021 | 0.9552 | 0.0117 | 0.0023 | 0.9860 | 0.9971 | 0.0029 |
| | 16 | 0.0405 | 0.0052 | 0.9543 | 0.0122 | 0.0050 | 0.9827 | 0.9927 | 0.0073 |
| | 17 | 0.0399 | 0.0047 | 0.9554 | 0.0125 | 0.0054 | 0.9821 | 0.9908 | 0.0092 |
| | 18 | 0.0378 | 0.0073 | 0.9549 | 0.0128 | 0.0075 | 0.9796 | 0.9899 | 0.0101 |
| | 19 | 0.0329 | 0.0120 | 0.9551 | 0.0136 | 0.0122 | 0.9742 | 0.9816 | 0.0184 |
| | 20 | 0.0303 | 0.0140 | 0.9557 | 0.0132 | 0.0137 | 0.9731 | 0.9800 | 0.0200 |
| | 21 | 0.0352 | 0.0096 | 0.9553 | 0.0130 | 0.0094 | 0.9776 | 0.9772 | 0.0228 |
| | 22 | 0.0256 | 0.0185 | 0.9559 | 0.0139 | 0.0137 | 0.9724 | 0.9344 | 0.0656 |
| | 23 | 0.0284 | 0.0163 | 0.9553 | 0.0143 | 0.0150 | 0.9707 | 0.9088 | 0.0912 |
| | 24 | 0.0237 | 0.0215 | 0.9549 | 0.0149 | 0.0151 | 0.9700 | 0.7042 | 0.2958 |
| | 25 | 0.0211 | 0.0233 | 0.9556 | 0.0148 | 0.0152 | 0.9700 | 0.6496 | 0.3504 |
| | 26 | 0.0191 | 0.0258 | 0.9551 | 0.0137 | 0.0152 | 0.9711 | 0.4353 | 0.5647 |
| | 27 | 0.0165 | 0.0279 | 0.9555 | 0.0130 | 0.0154 | 0.9716 | 0.3677 | 0.6323 |
| | 28 | 0.0143 | 0.0307 | 0.9550 | 0.0118 | 0.0152 | 0.9730 | 0.2232 | 0.7768 |
| | 29 | 0.0115 | 0.0329 | 0.9556 | 0.0098 | 0.0150 | 0.9752 | 0.1278 | 0.8722 |
| | 30 | 0.0091 | 0.0353 | 0.9556 | 0.0079 | 0.0151 | 0.9771 | 0.0699 | 0.9301 |
| | 31 | 0.0067 | 0.0380 | 0.9554 | 0.0058 | 0.0151 | 0.9791 | 0.0523 | 0.9477 |
| | 32 | 0.0047 | 0.0410 | 0.9544 | 0.0041 | 0.0148 | 0.9810 | 0.0378 | 0.9622 |
| | 33 | 0.0023 | 0.0423 | 0.9554 | 0.0022 | 0.0146 | 0.9832 | 0.0227 | 0.9773 |
| | 34 | 0.0000 | 0.0453 | 0.9547 | 0.0000 | 0.0145 | 0.9855 | 0.0000 | 1.0000 |
| 60 | 35 | 0.0431 | 0.0000 | 0.9569 | 0.0081 | 0.0000 | 0.9919 | 1.0000 | 0.0000 |
| | 36 | 0.0511 | 0.0027 | 0.9462 | 0.0084 | 0.0024 | 0.9892 | 0.9884 | 0.0116 |
| | 37 | 0.0420 | 0.0116 | 0.9464 | 0.0084 | 0.0113 | 0.9804 | 0.9793 | 0.0207 |
| | 38 | 0.0335 | 0.0203 | 0.9461 | 0.0087 | 0.0169 | 0.9745 | 0.8758 | 0.1242 |
| | 39 | 0.0281 | 0.0258 | 0.9461 | 0.0085 | 0.0172 | 0.9743 | 0.6912 | 0.3088 |
| | 40 | 0.0229 | 0.0310 | 0.9461 | 0.0090 | 0.0180 | 0.9730 | 0.5209 | 0.4791 |
| | 41 | 0.0172 | 0.0365 | 0.9463 | 0.0099 | 0.0189 | 0.9711 | 0.3452 | 0.6548 |
| | 42 | 0.0102 | 0.0447 | 0.9451 | 0.0080 | 0.0184 | 0.9736 | 0.1059 | 0.8941 |
| | 43 | 0.0054 | 0.0410 | 0.9536 | 0.0048 | 0.0169 | 0.9783 | 0.0485 | 0.9515 |
| | 44 | 0.0023 | 0.0517 | 0.9459 | 0.0019 | 0.0178 | 0.9803 | 0.0190 | 0.9810 |
| | 45 | 0.0000 | 0.0434 | 0.9566 | 0.0000 | 0.0193 | 0.9807 | 0.0000 | 1.0000 |

crystallizer should be operated at a higher temperature to deposit $C_{60}$-rich solid solution from the stream mixture, whereas the crystallization has to be run at a lower temperature if solids of $C_{70}$-rich solid solution are to be obtained.

## Synthesis of a Crystallization-Based Separation Process for Producing Pure $C_{60}$ and $C_{70}$ Solids

The flowsheet of a feasible crystallization-based separation process for the production of pure $C_{60}$ and $C_{70}$ solids from their mixture can be synthesized by constructing process paths on the phase diagram. To make it easier to follow, process paths are drawn on a sketch of the actual phase diagram in Figure 4a and the conceptual flowsheet is given in Figure 4b, where the stream numbers (enclosed in rectangles) correspond to the composition point numbers in Figure 4a.

The crystallization-based process requires two crystallizers (***20*** and ***40***), two solid/liquid (S/L) separators (***21*** and ***41***), two multistage crystallization units (***22*** and ***42***), two solvent-recovery units (***23*** and ***43***), and a solvent evaporator (***30***). It consists of two parts—fractionation of the $C_{60}$-$C_{70}$ fullerene mixture into $C_{60}$-rich and $C_{70}$-rich solid solutions, followed by purification of each of the enriched solid solutions with multistage crystallization into pure $C_{60}$ and $C_{70}$ solids, respectively. The feed solution (F) of mixed fullerenes in *o*-xylene is first combined with the recycle stream **5** to form stream **1**. As this stream has a much higher content of $C_{60}$ than $C_{70}$, crystallization of $C_{60}$-rich solid solution from the mixture is performed first. Therefore, stream **1** enters

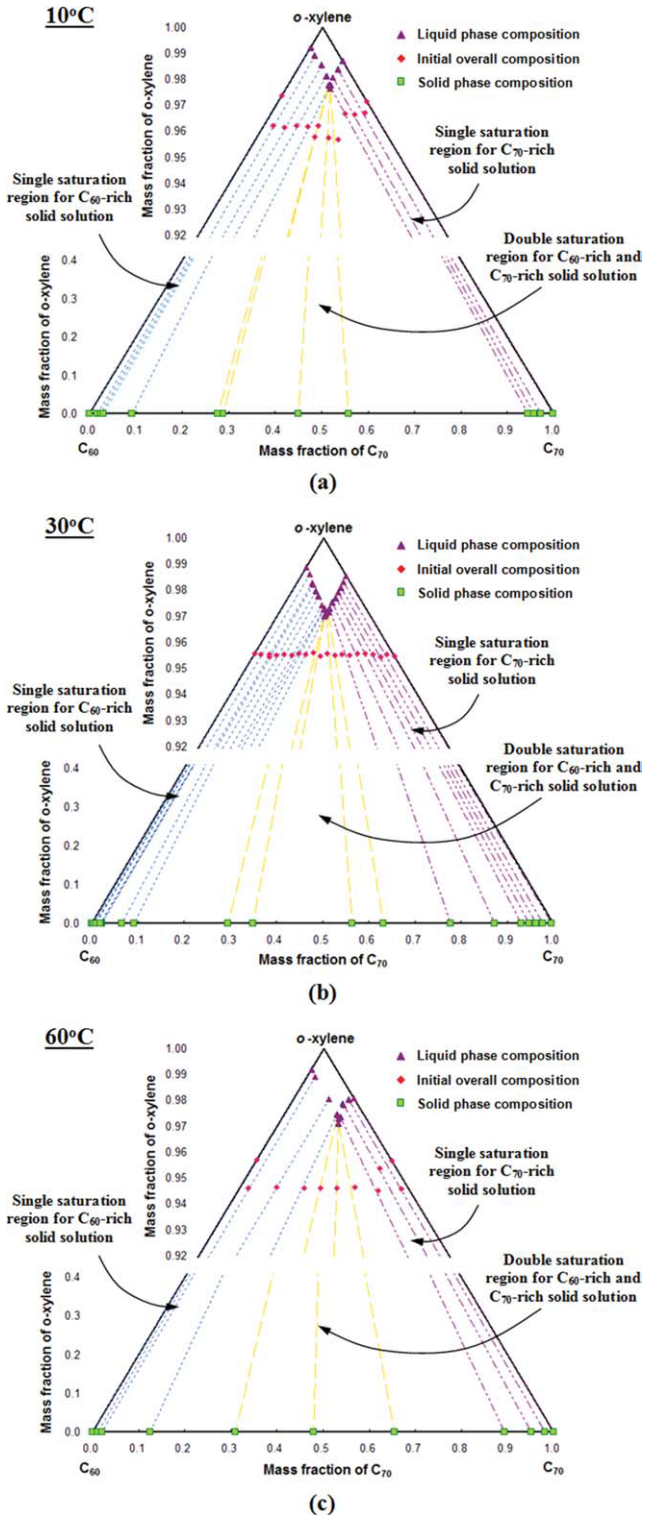


**Figure 2. Solid–liquid equilibrium phase diagram of the system $C_{60}$-$C_{70}$-*o*-xylene at (a) 10°C, (b) 30°C, and (c) 60°C.**

[Color figure can be viewed in the online issue, which is available at www.interscience.wiley.com.]

crystallizer ***20*** operating at a high temperature $T_h$ (Figure 4a). The solid crystals of $C_{60}$-rich solid solution (stream **6**) are then separated from the mother liquor (stream **2**) in the solid–liquid separator ***21***. After this, stream **2** is passed to the evaporator ***30***, where a suitable amount of *o*-xylene is removed to adjust the composition of the stream to point **3**. The resulting mixture enters crystallizer ***40*** operating at temperature $T_c$, where $T_c < T_h$. Under this condition, $C_{70}$-rich solid solution becomes supersaturated and crystals of a composition indicated by point **12** are formed. These solids are isolated from the mother liquor (stream **4**) in the solid–liquid separator ***41*** and form stream **12**. Stream **4** is then transferred to the mixer ***50***, in which it is combined with streams **11** and **17** from the multistage crystallization units ***22*** and ***42*** to produce stream **5**. This stream is recycled and mixed with the fresh feed F.

To convert the $C_{60}$-rich solid solution (stream **6**) and the $C_{70}$-rich solid solution (stream **12**) into pure $C_{60}$ and $C_{70}$ solids, respectively, multistage crystallization units involving either a train of crystallizers or a column crystallizer are used. Figure 5a displays a simplified isobaric–isothermal phase diagram of the system $C_{60}$-$C_{70}$-*o*-xylene, on which process paths are plotted to explain how a multistage crystallization unit purifies $C_{60}$-rich solid solutions into pure $C_{60}$ solids. Figure 5b portrays the corresponding process, which comprises three crystallizer and solid–liquid separator pairs that operate, in this example, at three different temperatures with $T_h > T_m > T_c$. The stream numbers (enclosed in rectangles) in the process flowsheet correspond to the composition point numbers in Figure 5a. The $C_{60}$-rich solid solution in stream **6** is mixed with the liquid stream **71** in crystallizer ***60*** at $T_h$. The resulting mixture undergoes a phase split along the tie-line (short-dashed line) ***a*** in Figure 5a to generate a $C_{60}$-enriched solid solution (stream **72**) and a liquid phase enriched in $C_{70}$ (stream **11**). The solid solution **72** is then transferred to crystallizer ***62*** to go through another crystallization at a lower temperature $T_m$ to obtain a solid phase further enriched in $C_{60}$ (point **74** in Figure 5a). Following this strategy, a highly pure $C_{60}$ (point **8**) can be obtained as the final product after mixing solid solution **74** with pure *o*-xylene in crystallizer ***64*** at $T_c$. Note that depending on the crystallization temperature(s), the purified $C_{60}$ solids may contain solvates.[34,35] To remove the solvate that may be present, the products from multistage crystallization unit are eventually directed to a solvent recovery unit such as a vacuum oven (***23*** in Figure 4b) so that high-purity $C_{60}$ solids can be produced. Pure $C_{70}$ solids can also be manufactured from $C_{70}$-rich solid solutions (stream **12**) using a similar multistage crystallization process (***42***) as described earlier, followed by the *o*-xylene removal unit (***43***).

## Batch Experiments to Produce Pure $C_{60}$ and $C_{70}$ Solids from a Commercial Fullerene Mixture

Two bench-scale batch experiments using different fullerene mixtures as feed materials were performed to validate the synthesized process and to demonstrate the detailed procedure of the separation process.

### *First separation experiment—using raw nanom-mix ST as feed materials*

The goal of the first set of experiments is to investigate whether the synthesized process succeeds in separating pure $C_{60}$ and $C_{70}$ solids from mixed fullerenes. The fullerene

**Table 2. Comparison of the Solvent-Free Composition of the Initial Mixture with that of the Liquid Phase and that of the Solid Phase for Each Set of SLE Data**

| | | Solvent-Free Composition of Initial Mixture (Mass Fraction) | | Solvent-Free Composition of Liquid Phase (Mass Fraction) | | Solvent-Free Composition of Solid Phase (Mass Fraction) | | |
|---|---|---|---|---|---|---|---|---|
| Temp. (°C) | Sample No. | $C_{60}$ | $C_{70}$ | $C_{60}$ | $C_{70}$ | $C_{60}$ | $C_{70}$ | Saturation Region of |
| 10 | 1 | 1.0000 | 0.0000 | 1.0000 | 0.0000 | 1.0000 | 0.0000 | $C_{60}$-rich solid solution |
| | 2 | 0.9261 | 0.0739 | 0.7491 | 0.2509 | 0.9828 | 0.0172 | |
| | 3 | 0.8228 | 0.1772 | 0.5348 | 0.4652 | 0.9763 | 0.0237 | |
| | 4 | 0.7283 | 0.2717 | 0.4429 | 0.5571 | 0.9699 | 0.0301 | |
| | 5 | 0.6244 | 0.3756 | 0.3881 | 0.6119 | 0.9093 | 0.0907 | |
| | 6 | 0.5601 | 0.4399 | 0.4074 | 0.5926 | 0.7239 | 0.2761 | $C_{60}$-rich solid solution + |
| | 7 | 0.5377 | 0.4623 | 0.4174 | 0.5826 | 0.7121 | 0.2879 | $C_{70}$-rich solid solution |
| | 8 | 0.4543 | 0.5457 | 0.3978 | 0.6022 | 0.5504 | 0.4496 | |
| | 9 | 0.3888 | 0.6112 | 0.3962 | 0.6038 | 0.4420 | 0.5580 | |
| | 10 | 0.2835 | 0.7165 | 0.4111 | 0.5889 | 0.0561 | 0.9439 | $C_{70}$-rich solid solution |
| | 11 | 0.2000 | 0.8000 | 0.3286 | 0.6714 | 0.0421 | 0.9579 | |
| | 12 | 0.0909 | 0.9091 | 0.1897 | 0.8103 | 0.0272 | 0.9728 | |
| | 13 | 0.0000 | 1.0000 | 0.0000 | 1.0000 | 0.0000 | 1.0000 | |
| 30 | 14 | 1.0000 | 0.0000 | 1.0000 | 0.0000 | 1.0000 | 0.0000 | $C_{60}$-rich solid solution |
| | 15 | 0.9533 | 0.0467 | 0.8345 | 0.1655 | 0.9971 | 0.0029 | |
| | 16 | 0.8872 | 0.1128 | 0.7084 | 0.2916 | 0.9927 | 0.0073 | |
| | 17 | 0.8942 | 0.1058 | 0.6962 | 0.3038 | 0.9908 | 0.0092 | |
| | 18 | 0.8384 | 0.1616 | 0.6302 | 0.3698 | 0.9899 | 0.0101 | |
| | 19 | 0.7330 | 0.2670 | 0.5279 | 0.4721 | 0.9816 | 0.0184 | |
| | 20 | 0.6832 | 0.3168 | 0.4921 | 0.5079 | 0.9800 | 0.0200 | |
| | 21 | 0.7862 | 0.2138 | 0.5811 | 0.4189 | 0.9772 | 0.0228 | |
| | 22 | 0.5801 | 0.4199 | 0.5033 | 0.4967 | 0.9344 | 0.0656 | |
| | 23 | 0.6357 | 0.3643 | 0.4868 | 0.5132 | 0.9088 | 0.0912 | |
| | 24 | 0.5247 | 0.4753 | 0.4965 | 0.5035 | 0.7042 | 0.2958 | $C_{60}$-rich solid solution + |
| | 25 | 0.4757 | 0.5243 | 0.4940 | 0.5060 | 0.6496 | 0.3504 | $C_{70}$-rich solid solution |
| | 26 | 0.4245 | 0.5755 | 0.4727 | 0.5273 | 0.4353 | 0.5647 | |
| | 27 | 0.3720 | 0.6280 | 0.4591 | 0.5409 | 0.3677 | 0.6323 | |
| | 28 | 0.3172 | 0.6828 | 0.4363 | 0.5637 | 0.2232 | 0.7768 | $C_{70}$-rich solid solution |
| | 29 | 0.2595 | 0.7405 | 0.3960 | 0.6040 | 0.1278 | 0.8722 | |
| | 30 | 0.2053 | 0.7947 | 0.3427 | 0.6573 | 0.0699 | 0.9301 | |
| | 31 | 0.1492 | 0.8508 | 0.2758 | 0.7242 | 0.0523 | 0.9477 | |
| | 32 | 0.1028 | 0.8972 | 0.2181 | 0.7819 | 0.0378 | 0.9622 | |
| | 33 | 0.0510 | 0.9490 | 0.1285 | 0.8715 | 0.0227 | 0.9773 | |
| | 34 | 0.0000 | 1.0000 | 0.0000 | 1.0000 | 0.0000 | 1.0000 | |
| **60** | 35 | 1.0000 | 0.0000 | 1.0000 | 0.0000 | 1.0000 | 0.0000 | $C_{60}$-rich solid solution |
| | 36 | 0.9500 | 0.0500 | 0.7803 | 0.2197 | 0.9884 | 0.0116 | |
| | 37 | 0.7831 | 0.2169 | 0.4256 | 0.5744 | 0.9793 | 0.0207 | |
| | 38 | 0.6224 | 0.3776 | 0.3398 | 0.6602 | 0.8758 | 0.1242 | |
| | 39 | 0.5219 | 0.4781 | 0.3316 | 0.6684 | 0.6912 | 0.3088 | $C_{60}$-rich solid solution + |
| | 40 | 0.4251 | 0.5749 | 0.3342 | 0.6658 | 0.5209 | 0.4791 | $C_{70}$-rich solid solution |
| | 41 | 0.3203 | 0.6797 | 0.3441 | 0.6559 | 0.3452 | 0.6548 | |
| | 42 | 0.1850 | 0.8150 | 0.3026 | 0.6974 | 0.1059 | 0.8941 | $C_{70}$-rich solid solution |
| | 43 | 0.1163 | 0.8837 | 0.2215 | 0.7785 | 0.0485 | 0.9515 | |
| | 44 | 0.0430 | 0.9570 | 0.0959 | 0.9041 | 0.0190 | 0.9810 | |
| | 45 | 0.0000 | 1.0000 | 0.0000 | 1.0000 | 0.0000 | 1.0000 | |

mixture, namely, nanom-mix ST (Frontier Carbon Corporation), was used as the feed materials for the experiment. According to the supplier, this mixture contains 60 wt % $C_{60}$, 25 wt % $C_{70}$, and 15 wt % higher fullerenes. The temperatures selected for performing the crystallization of $C_{60}$-rich and $C_{70}$-rich solid solutions were 110 and $-16$°C, respectively. These values were selected based on considerations related to the boiling and freezing points of *o*-xylene, the heating or cooling capacity of the equipment available, and the desire to accomplish the separation of pure $C_{60}$ and $C_{70}$ solids with the smallest number of crystallization steps.

The procedure of this separation experiment is captured on a schematic phase diagram and a process flow diagram displayed in Figure 6. Note that the phase diagram in Figure 6a is intended for illustrative purpose only, and the composition points on the diagram do not represent the actual experimental results. To prepare feed materials for the process, 25 g of nanom-mix was stirred with 750 g of *o*-xylene (purity 97%, Aldrich) in a 1-L conical flask at room temperature for 3 days. After filtering out the solids that did not dissolve, a 600.12 g solution of mixed fullerenes comprising 67.57 wt % of $C_{60}$ and 32.43 wt % of $C_{70}$ was obtained (Point **1**)

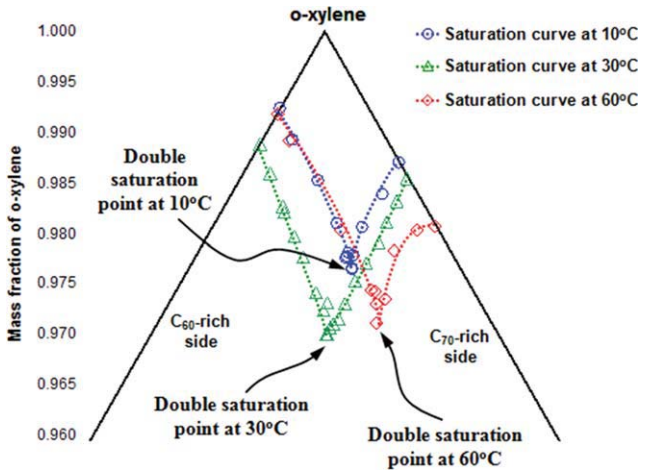


**Figure 3. Solid–liquid saturation curves of the system $C_{60}$-$C_{70}$-*o*-xylene at 10°, 30°C, and 60°C.**

[Color figure can be viewed in the online issue, which is available at www.interscience.wiley.com.]

(Unless otherwise stated, the wt % given in this and in the coming sections are the relative wt % between $C_{60}$ and $C_{70}$ calculated on a solvent-free basis). This solution was placed in a 1-L erlenmeyer flask, which was then immersed in an oil bath to undergo the first crystallization step of $C_{60}$-rich solid solution. A hot plate-magnetic stirrer (Heidolph, model MR 3001K) and a temperature controller (Heidolph, model EKT 3001) were used to maintain the fullerene solution at 110°C and to keep it stirred for 1 day. At such a high temperature, the solution was supersaturated with $C_{60}$-rich solid solution so that a solid and a liquid phase of compositions **1S** and **1L** (Figure 6a), respectively, were produced. The solid crystals were then isolated from the mother liquor by suction filtration with a fritted-disc filtering funnel. HPLC analyses (using the same equipment and operating conditions as that for determining the SLE phase diagram) revealed that the solid phase **1S** contained 93.91 wt % $C_{60}$ and 6.09 wt % $C_{70}$, whereas the mother liquor **1L** had a composition of 47.08 wt % $C_{60}$ and 52.92 wt % $C_{70}$. Compared with the composition of $C_{60}$ in the initial fullerene solution (67.57 wt %), it was obvious that the solid phase was much more enriched in $C_{60}$ subsequent to the first crystallization. After this point, the experimental run proceeded in two different directions. In one direction, part of the collected solid phase **1S** was mixed with a proper amount of fresh *o*-xylene to make up a supersaturated slurry mixture consisting of about 5 wt % (actual wt %) fullerene solids (Point **2**). This mixture was stirred at 110°C for 1 day using the same setup described earlier to go through the second crystallization step of $C_{60}$-rich solid solution, from which a liquid phase **2L** and a solid phase **2S** were generated. The crystals from **2S** were subjected to two more similar crystallization steps at 110°C to obtain fullerene solids **4S**. A total of 2.14 g of solids comprising 96.97 wt % $C_{60}$ were finally obtained after solid phase **4S** was dried in a vacuum oven at 30°C for 1 day to get rid of the solvent. The second column of Table 3 records the $C_{60}$ composition of the solid phase obtained after each of the four crystallization steps for the $C_{60}$-rich solid solution.

In the other direction, the mother liquor **1L** was concentrated using a rotary evaporator (Heidolph, model Laborota 4011 digital), by which 241.71 g of *o*-xylene was removed from the solution. The resulting mixture (point **5**) was transferred to a media bottle and then cooled in a freezer to −16°C for 1 day without mixing to undergo the first crystallization step of $C_{70}$-rich solid solution. From this step, a liquid phase **5L** and a solid phase **5S** were generated. The $C_{70}$ composition in the solid phase **5S** was enhanced from 52.92 wt % in mother liquor **1L** to 77.7 wt % by crystallization. Part of the solid crystals **5S** obtained was then mixed with fresh *o*-xylene to prepare a slurry solution comprising 5 wt % (actual wt %) of fullerene solids (Point **6**). In the second crystallization of $C_{70}$-rich solid solution, this mixture was, again, kept at −16°C in the freezer for 1 day without mixing to allow the formation of the liquid phase **6L** and the solid phase **6S**. Two more crystallization operations at −16°C were performed to increase the $C_{70}$ content in the solid phase **6S** to the composition represented by **8S**. To remove

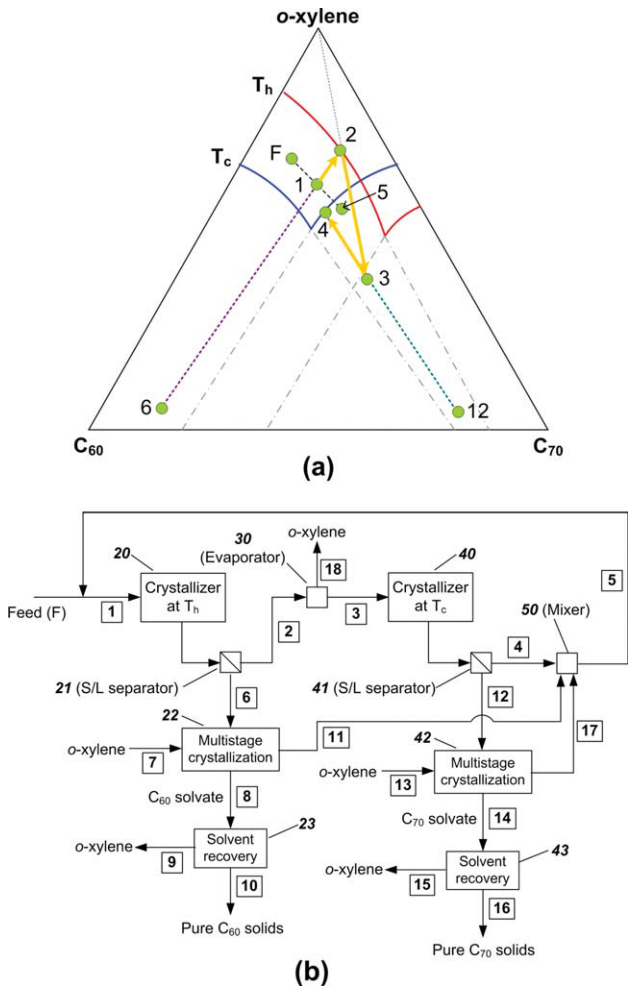


**Figure 4. Synthesis of the crystallization-based separation process for the production of pure $C_{60}$ and $C_{70}$ solids.**

(a) A schematic phase diagram with process paths to illustrate movements in composition space; (b) the corresponding process flowsheet. [Color figure can be viewed in the online issue, which is available at www.interscience.wiley.com.]

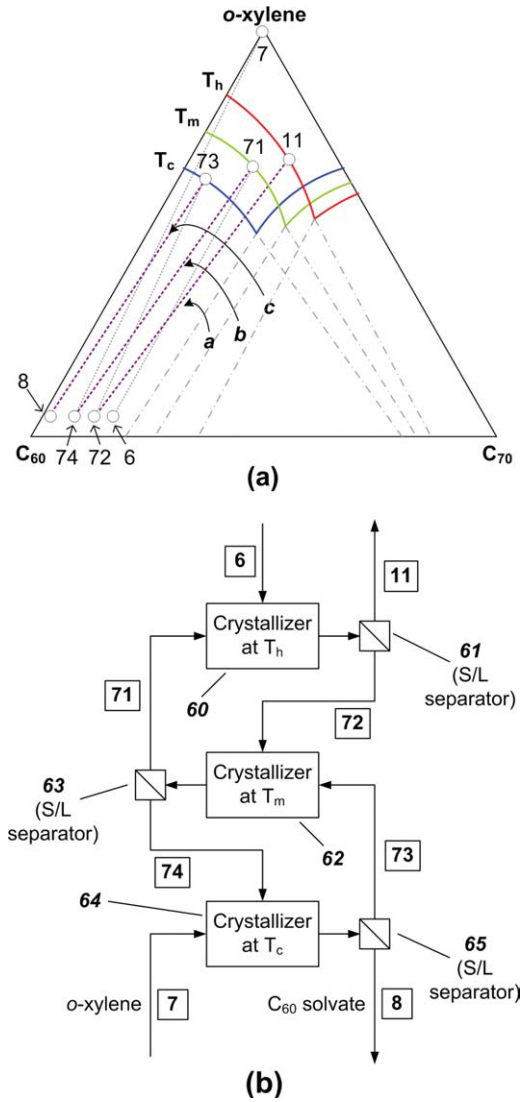


**Figure 5. Operation of the multistage crystallization unit for converting $C_{60}$-rich solid solution into pure $C_{60}$ solids.**

(a) A schematic phase diagram with process paths to illustrate movements in composition space; (b) the corresponding process flowsheet. [Color figure can be viewed in the online issue, which is available at www.interscience.wiley.com.]

the solvent, solids **8S** were vacuum dried at 30°C for 1 day, and 1.09 g fullerene $C_{70}$ solids of 98.07 wt % purity were eventually acquired. The $C_{70}$ compositions of the solid phases generated from the four crystallization steps of $C_{70}$-rich solid solution are listed in the third column of Table 3.

Based on the results from this separation experiment, it could be confirmed that, in principle, the proposed crystallization-based separation process succeeded in producing both pure $C_{60}$ and $C_{70}$ solids from mixed fullerenes. However, two problems on the quality of the fullerene products were found. First, it was observed that a portion of the fullerene solids collected from the crystallization steps operated at 110°C could not redissolve in toluene or in *o*-xylene even after they were agitated in a large amount of solvent for a week. Such insoluble solids were very fine black powder and they were believed to be formed from the degradation of fullerenes after prolonged exposure in an environment of high temperature. HPLC chromatograms of those mother liquors obtained from the crystallization steps at 110°C also exhibited numerous absorption peaks of unknown species. Hence, to prevent the degradation of fullerenes and to increase the yield of the fullerene products, the crystallization steps for enriching $C_{60}$ in the solid phases had to be done at a lower temperature and with shorter duration. Second, based on HPLC results, the majority of higher fullerenes originated from the feed materials were found to deposit together with the $C_{70}$-rich solid solutions in the crystallization steps at −16°C. This means that the solubility behavior of higher fullerenes is similar to that of $C_{70}$, and thus such higher fullerenes cannot be removed from the $C_{70}$ products simply by crystallization at the currently selected operating conditions.

### *Second separation experiment—using pretreated nanom-mix ST as feed materials*

To overcome the problems encountered in the first experiment, two changes were made. The first one was to use a pretreated nanom-mix solution from which higher fullerenes had been removed as the feed materials. The second modification was to reduce the operating temperature and duration of the crystallization steps for $C_{60}$-rich solid solution from 110°C and 1 day to 90°C and 10 h, respectively.

The higher fullerenes in nanom-mix were removed using a liquid chromatographic (LC) column packed with activated carbon as adsorbents. The glass column had dimensions of 45 cm long × 6 cm I.D. A coarse fritted disc for supporting the adsorbents was fused near the bottom of the column. A stopcock (straight bore, Teflon plug) was also installed at the bottom end of the column for regulating the flow rate during elution. The activated carbon (Filtrasorb® F400, Calgon Carbon Corporation) was pretreated as follows. First, they were sieved to get rid of the fine powder and ash. Next, the sieved adsorbents were heated in an oven at 100°C for 1 day to eliminate the moisture. The dried activated carbon was then immersed in *o*-xylene (purity 97%, Aldrich) for 1 night to remove the trapped air bubbles. To pack the adsorbents, cotton was first placed on top of the fritted disc in the column, followed by a layer of sea sand (acid washed and calcined, RDH). About 500 g of the pretreated activated carbon was then used to form the packed bed. Finally, another layer of sea sand was put on top of the packed bed to complete the LC column assembly.

To prepare the nanom-mix solution for pretreatment, 28 g of nanom-mix solids were mixed with 1 L of *o*-xylene in a media bottle for 2 days. After filtering out the excess solids, the resulting fullerene mixture solution was diluted with 6 L of pure *o*-xylene. According to HPLC analyses, the $C_{60}$ and $C_{70}$ concentrations in such a diluted solution were about 1.75 and 0.65 g/L, respectively. The pretreatment process was executed by continuously feeding this solution into the LC column with the flow rate of elution set at about 1 mL/min. As the activated carbon was found in preliminary studies to have an affinity to adsorb fullerene species in the order of $C_{60} < C_{70} <$ higher fullerenes, $C_{60}$ would breakthrough from the column first, followed by $C_{70}$, and then the

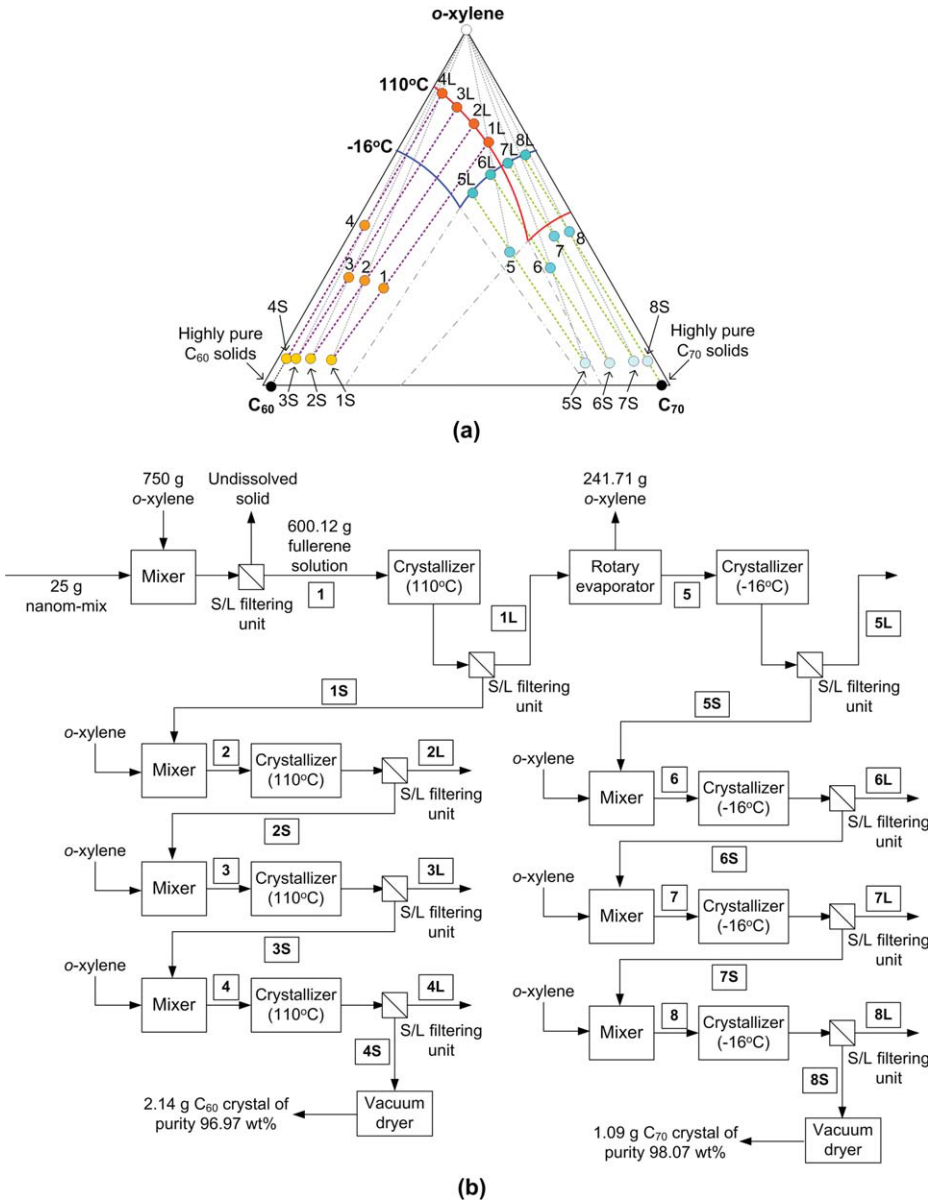


**Figure 6. Procedure of the first separation experiment.**

(a) A schematic phase diagram with process paths to illustrate movements in composition space; (b) the corresponding process flow diagram. [Color figure can be viewed in the online issue, which is available at www.interscience.wiley.com.]

higher fullerenes. This sequence is illustrated graphically in Figure 7. The fraction used for the crystallization process is the one containing $C_{60}$ and $C_{70}$ only. If any higher fullerenes were detected by HPLC in the effluent, the maximum adsorption capacity of the packing materials had been reached and the column process was stopped. Using the

**Table 3. $C_{60}$ or $C_{70}$ Composition of the Solid Phase after Each Crystallization Step in the First Separation Experiment**

| | $C_{60}$ Composition in Solid Phase—Crystallization of $C_{60}$-Rich Solid Solution at 110°C (Relative wt % Between $C_{60}$ and $C_{70}$ on Solvent-Free Basis) | $C_{70}$ Composition in Solid Phase—Crystallization of $C_{70}$-Rich Solid Solution at −16°C (Relative wt % Between $C_{60}$ and $C_{70}$ on Solvent-Free Basis) |
|---|---|---|
| After first crystallization | 93.91 (Point/stream **1S**) | 77.7 (Point/stream **5S**) |
| After second crystallization | 96.03 (Point/stream **2S**) | 83.11 (Point/stream **6S**) |
| After third crystallization | 96.84 (Point/stream **3S**) | 94.99 (Point/stream **7S**) |
| After fourth crystallization | 96.97 (Point/stream **4S**) | 98.07 (Point/stream **8S**) |

Refer to Figure 6 for point/stream numbers.

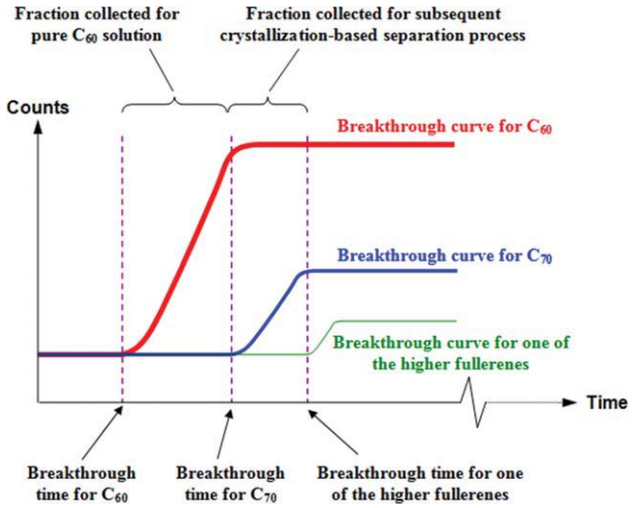


**Figure 7. Breakthrough curves of different fullerene species from the LC column with the nanom-mix solution being fed continuously.**

[Color figure can be viewed in the online issue, which is available at www.interscience.wiley.com.]

equipment and operating conditions specified, a typical LC column run could treat about 6.5 L of the prepared nanom-mix solution and produced a binary fullerene mixture consisting of 8.5–9 g of $C_{60}$ and 1.4–1.5 g of $C_{70}$.

In the second separation experiment, the feed was a fullerene solution containing 16.05 g of $C_{60}$ and 3.32 g of $C_{70}$ dissolved in 1419.12 g of *o*-xylene (i.e., initial composition: 82.8 wt % $C_{60}$ and 17.2 wt % $C_{70}$), which was the product obtained by running two batches of LC column pretreatment of nanom-mix solution. Figure 8 illustrates the procedure for this experiment with the aid of a schematic phase diagram and a process flow diagram. In general, the second separation process was executed in a similar manner as that in the first experiment, except for three minor practices as described in the following.

First of all, as the feed materials had a high composition of $C_{60}$, after the first crystallization step of $C_{60}$-rich solid solution at 90°C, it was noticed that mother liquor **1L** was not adequately enriched in $C_{70}$ (composition: 71.87 wt % $C_{60}$, 28.13 wt % $C_{70}$) (Table 4), and its composition could not enter the single saturation region of $C_{70}$-rich solid solution even after solvent removal and cooling. Therefore, two additional sets of operations incorporating both solvent removal and crystallization at 90°C were performed to generate mother liquor **3L**, which was much richer in $C_{70}$ (composition: 33.41 wt % $C_{60}$ and 66.59 wt % $C_{70}$) (Table 4). Note that in this case, the crystallization steps for slurry mixtures **2** and **3** were not intended for purifying the $C_{60}$ solids but for enriching the $C_{70}$ content in the liquid phase. Liquid phase **3L**, after undergoing one more solvent-removal step in the rotary evaporator, was ready for the crystallization at −16°C to separate $C_{70}$-rich solid solution from the mixture (stream/point **6** in Figure 8).

Second, again, as the feed materials were originally rich in $C_{60}$, the solid phases **1S**, **2S**, and **3S** formed from the first three crystallization steps at 90°C also possessed high concentrations of $C_{60}$ (93–97 wt %, Table 4). It was thus more economical to combine these streams and then purify the resulting solid mixture using two more crystallization steps at 90°C.

The third practice that made the procedure of the second experiment different from that of the first one was the manner in which the crystallization steps at −16°C were performed. Recall that in the first experiment, crystallization was effected by putting the $C_{70}$-rich slurry mixture or solution in a freezer without mixing for a day. To enhance the rate to reach equilibrium, in the second experiment, before the freshly prepared slurry mixture was placed inside the freezer, it was first magnetically stirred at room temperature for about 1 h to allow an intimate contact between the fullerene solids and *o*-xylene.

Table 4 summarizes the solvent-free compositions of both the solid and liquid phases formed from each crystallization step in this experiment. A total of 10.78 g $C_{60}$ crystals of purity 99.4 wt % and 1.15 g $C_{70}$ solids of purity 99.1 wt % were finally obtained. In terms of the mass ratio of pure $C_{60}$ solids produced from the process to $C_{60}$ solids present in the feed of the crystallization process, the single-pass yield of $C_{60}$ in this experiment was 0.672. Using similar definition, the yield of $C_{70}$ was 0.346. By comparing the data in Table 3 with those in Table 4, we could see that after higher fullerenes were taken away from the feed materials, the efficiency of each crystallization step on enriching the $C_{60}$ or $C_{70}$ content in the solid phases was improved. Moreover, after reducing the temperature and duration for the crystallization of $C_{60}$-rich solid solution, the solids acquired readily dissolved in toluene or *o*-xylene to form clear solutions. This showed that the problem of fullerene degradation had been eliminated. This was further supported by the HPLC chromatograms of the relevant solid and liquid phases, from which no peaks of unknown identities were observed.

## Conclusions

With the experimental solid–liquid equilibrium phase diagram of the system $C_{60}$-$C_{70}$-*o*-xylene, a crystallization-based process that separates pure fullerenes $C_{60}$ and $C_{70}$ solids from their mixture using *o*-xylene as the solvent has been synthesized in this study. As $C_{60}$ and $C_{70}$ were found to form solid solutions over certain composition range and the solvent-free composition of $C_{60}$-$C_{70}$ double saturation point changed with temperature, the process was designed to consist of two major parts. The first part was the fractionation of the $C_{60}$-$C_{70}$ mixture into $C_{60}$-rich and $C_{70}$-rich solid solutions using temperature-swing crystallization. These two solid solutions were then purified by multistage crystallization to yield pure $C_{60}$ and $C_{70}$ solids, respectively. Using this process, we demonstrated that $C_{60}$ and $C_{70}$ solids of purity greater than 99 wt % could be produced from a commercial fullerene mixture that was pretreated with adsorption to remove higher fullerenes.

Compared with liquid chromatography, the crystallization process we have developed has considerable potential of separating fullerenes commercially at a lower cost. To further enhance its economical potential, the crystallization process can be optimized by adjusting the operating temperature and amount of solvents used for the crystallization steps, rearranging the process streams, and replacing the costly

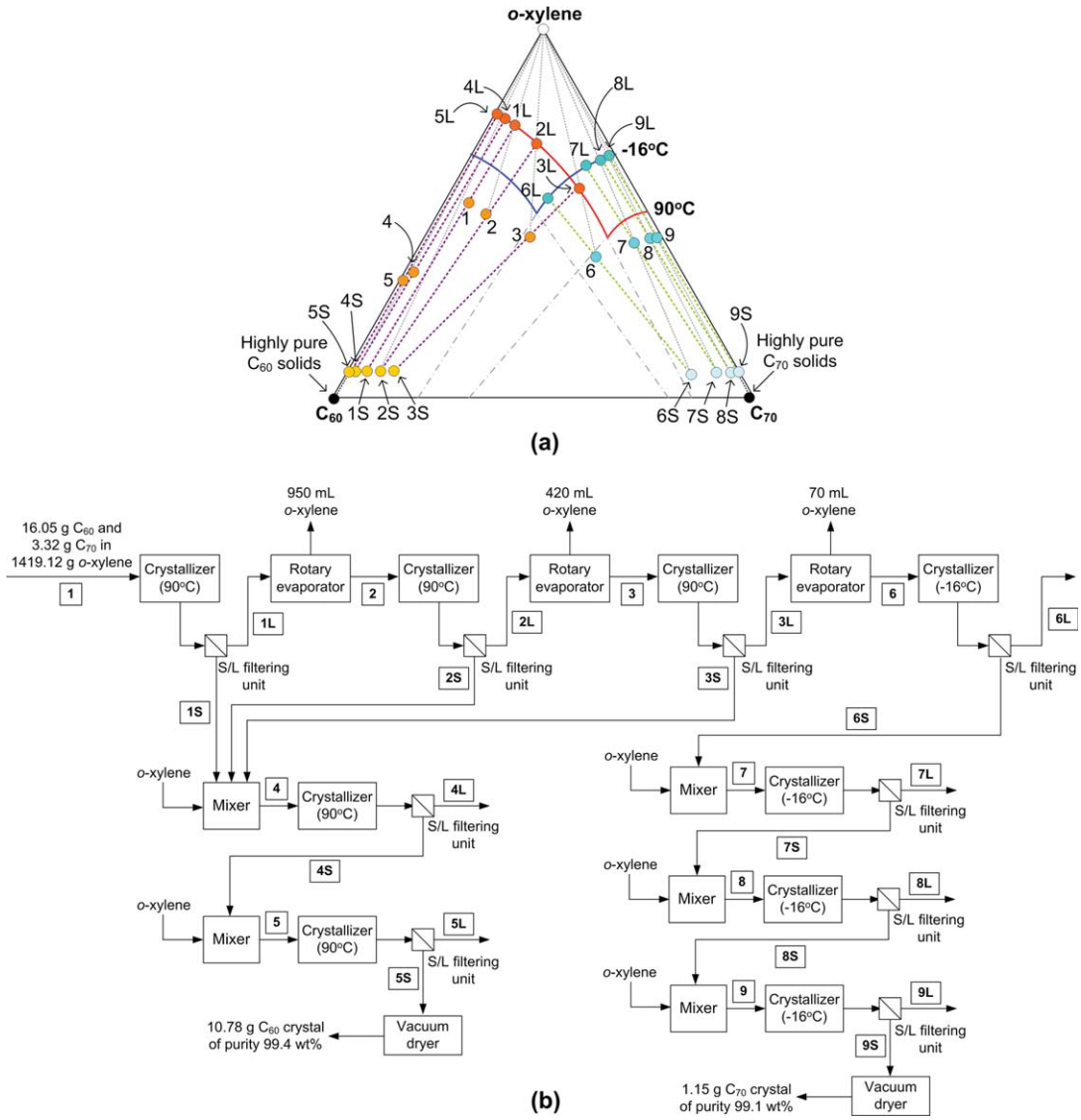


**Figure 8. Procedure of the second separation experiment.**

(a) A schematic phase diagram with process paths to illustrate movements in composition space; (b) the corresponding process flow diagram. [Color figure can be viewed in the online issue, which is available at www.interscience.wiley.com.]

**Table 4. Compositions of Both the Solid and Liquid Phases Formed from Each Step of Crystallization in the Second Separation Experiment**

| | Composition of Liquid Phase (Relative wt % Between $C_{60}$ and $C_{70}$ on Solvent-Free Basis) | | | Composition of Solid Phase (Relative wt % Between $C_{60}$ and $C_{70}$ on Solvent-Free Basis) | | |
|---|---|---|---|---|---|---|
| Crystallization no. | Point or Stream No. | $C_{60}$ | $C_{70}$ | Point or Stream No. | $C_{60}$ | $C_{70}$ |
| 1 | **1L** | 71.87 | 28.13 | **1S** | 97.28 | 2.72 |
| 2 | **2L** | 53.04 | 46.96 | **2S** | 96.38 | 3.62 |
| 3 | **3L** | 33.41 | 66.59 | **3S** | 93.64 | 6.36 |
| 4 | **4L** | 79.23 | 20.77 | **4S** | 98.89 | 1.11 |
| 5 | **5L** | 94.73 | 5.27 | **5S** | 99.44 | 0.56 |
| 6 | **6L** | 62.10 | 37.90 | **6S** | 10.74 | 89.26 |
| 7 | **7L** | 50.17 | 49.83 | **7S** | 4.54 | 95.46 |
| 8 | **8L** | 36.73 | 63.27 | **8S** | 2.10 | 97.90 |
| 9 | **9L** | 23.67 | 76.33 | **9S** | 0.90 | 99.10 |

Refer to Figure 8 for point/stream numbers.

multistage crystallization with a single-column crystallizer.[36] Although the process presented here is only for the production of pure $C_{60}$ and $C_{70}$ solids, using the same synthesis principle, it can be extended to recover higher fullerenes such as $C_{84}$. Efforts in these directions are in progress.

## Acknowledgments

Financial support from the Research Grants Council (HKUST618106) is gratefully acknowledged. The authors thank Dr. Alex H. C. Chan, Mr. Sze K. Tam, and Mr. Yeuk T. Lau for their assistance in part of the experimental work.

## Literature Cited

1. Wienk MM, Kroon JM, Verhees WJH, Knol J, Hummelen JC, Van Hal PA, Janssen RAJ. Efficient methanol[70]fullerene/MDMO-PPV bulk heterojunction photovoltaic cells. *Angew Chem Int Ed*. 2003; 42:3371–3375.
2. Reyes-Reyes M, Kim K, Carroll DL. High-efficiency photovoltaic devices based on annealed poly(3-hexylthiophene) and 1-(3-methoxycarbonyl)-propyl-1-phenyl-(6,6)$C_{61}$ blends. *Appl Phys Lett*. 2005; 87:083506.
3. Sivula K, Ball ZT, Watanabe N, Fréchet JMJ. Amphiphilic diblock copolymer compatibilizers and their effect on the morphology and performance of polythiophene: Fullerene solar cells. *Adv Mater*. 2006;18:206–210.
4. Thompson BC, Frechet JMJ. Organic photovoltaics—polymer-fullerene composite solar cells. *Angew Chem Int Ed*. 2008;47:58–77.
5. Zakharian TY, Seryshev A, Sitharaman B, Gilbert BE, Knight V, Wilson LJ. A fullerene-paclitaxel chemotherapeutic: synthesis, characterization, and study of biological activity in tissue culture. *J Am Chem Soc*. 2005;127:12508–12509.
6. Dugan LL, Lovett EG, Quick KL, Lotharius J, Lin TT, O'Malley KL. Fullerene-based antioxidants and neurodegenerative disorders. *Parkinsonism Relat Disord*. 2001;7:243–246.
7. Schuster DI, Wilson SR, Schinazi RF. Anti-human immunodeficiency virus activity and cytotoxicity of derivatized buckminsterfullerenes. *Bioorg Med Chem Lett*. 1996;6:1253–1256.
8. Mashino T, Okuda K, Hirota T, Hirobe M. Inhibition of *E. coli* growth by fullerene derivatives and inhibition mechanism. *Bioorg Med Chem Lett*. 1999;9:2959–2962.
9. Tabata Y, Ikada Y. Biological functions of fullerene. *Pure Appl Chem*. 1999;71:2047–2053.
10. Bolskar RD, Benedetto AF, Husebo La, Price RE, Jackson EF, Wallace S, Wilson LJ, Alford JM. First soluble M@$C_{60}$ derivatives provide enhanced access to metallofullerenes and permit in vivo evaluation of Gd@$C_{60}[C(COOH)_2]_{10}$ as a MRI contrast agent. *J Am Chem Soc*. 2003;125:5471–5478.
11. Brusatin G, Signorini R. Linear and nonlinear optical properties of fullerenes in solid state materials. *J Mater Chem*. 2002;12:1964–1977.
12. Loutfy RO, Lowe TP, Moravsky AP, Katagiri S. *Commercial production of fullerenes and carbon nanotubes*. In: Osawa E, editor. *Perspectives of Fullerene Nanotechnology*. Dordrecht, The Netherlands: Kluwer Academic Publishers, 2002:35–46.
13. Grushko YS, Sedov VP, Shilin VA. Technology for manufacture of pure fullerenes $C_{60}$, $C_{70}$ and a concentrate of higher fullerenes. *Russ J Appl Chem*. 2007;80:448–455.
14. Howard JB, Lafleur AL, Makarovsky Y, Mitra S, Pope CJ, Yadav TK. Fullerenes synthesis in combustion. *Carbon*. 1992;30:1183–1201.
15. Takehara H, Fujiwara M, Arikawa M, Diener MD, Alford JM. Experimental study of industrial scale fullerene production by combustion synthesis. *Carbon*. 2005;43:311–319.
16. Darwish AD, Kroto HW, Taylor R, Walton DRM. Improved chromatographic-separation of $C_{60}$ and $C_{70}$. *J Chem Soc Chem Commun*. 1994; 15–16.
17. Jinno K,editor. *Separation of Fullerenes by Liquid Chromatography*. Cambridge: Royal Society of Chemistry, 1999.
18. Wang H, Lam FLY, Hu X, Ng KM. Ordered mesoporous carbon as an efficient and reversible adsorbent for the adsorption of fullerenes. *Langmuir*. 2006;22:4583–4588.
19. Atwood JL, Koutsantonis GA, Raston CL. Purification of $C_{60}$ and $C_{70}$ by selective complexation with calixarenes. *Nature*. 1994;368: 229–231.
20. Komatsu N. Preferential precipitation of $C_{70}$ over $C_{60}$ with *p*-halohomooxa-calix[3]arenes. *Org Biomol Chem*. 2003;1:204–209.
21. Murayama H, Tomonoh S, Alford JM, Karpuk ME. Fullerene production in tons and more: from science to industry. *Fullerene Nanotube Carbon Nanostruct*. 2004;12:1–9.
22. Coustel N, Bernier P, Aznar R, Zahab A, Lambert JM, Lyard P. Purification of $C_{60}$ by a simple crystallization procedure. *J Chem Soc Chem Commun*. 1992; 1402–1403.
23. Zhou XH, Gu ZN, Wu YQ, Sun YL, Jin ZX, Xiong Y, Sun BY, Wu Y, Fu H, Wang JZ. Separation of $C_{60}$ and $C_{70}$ fullerenes in gram quantities by fractional crystallization. *Carbon*. 1994;32:935–937.
24. Wu Y, Sun Y, Gu Z, Zhou X, Xiong Y, Sun B, Jin Z. A combined recrystallization and preparative liquid-chromatographic method for the isolation of pure $C_{70}$ fullerene. *Carbon*. 1994;32:1180–1182.
25. Doome RJ, Fonseca A, Richter H, Nagy JB, Thiry PA, Lucas AA. Purification of $C_{60}$ by fractional crystallization. *J Phys Chem Solids*. 1997;58:1839–1843.
26. Kwok KS, Chan HC, Chan CK, Ng KM. Experimental determination of solid-liquid equilibrium phase diagrams for crystallization-based process synthesis. *Ind Eng Chem Res*. 2005;44:3788–3798.
27. Kwok KS, Ng KM, Taboada ME, Cisternas LA. Thermodynamics of salt lake system: representation, experiments, and visualization. *AIChE J*. 2008;54:706–727.
28. Samant KD, Berry DA, Ng KM. Representation of high-dimensional, molecular solid-liquid phase diagrams. *AIChE J*. 2000;46: 2435–2455.
29. Dye SR, Ng KM. Fractional crystallization: design alternatives and tradeoffs. *AIChE J*. 1995;41:2427–2438.
30. Wibowo C, Ng KM. Visualization of high-dimensional phase diagrams of molecular and ionic mixtures. *AIChE J*. 2002;48:991–1000.
31. Wibowo C, Ng KM. Unified approach for synthesizing crystallization-based separation processes. *AIChE J*. 2000;46:1400–1421.
32. Lin SW, Ng KM, Wibowo C. Synthesis of crystallization processes for systems involving solid solutions. *Comput Chem Eng*. 2008;32: 956–970.
33. Zhou X, Liu J, Jin Z, Gu Z, Wu Y, Sun Y. Solubility of fullerene $C_{60}$ and $C_{70}$ in toluene, *o*-xylene and carbon disulfide at various temperatures. *Fuller Sci Technol*. 1997;5:285–290.
34. Arapov OV, Aksel'rod BM, Pronkin AA, Charykov NA, Ryazanova OY. Solubility in the fullerene $C_{60}$-fullerene $C_{70}$-*o*-$C_6H_4(CH_3)_2$ system. *Russ J Appl Chem*. 2003;76:33–36.
35. Ponomarev AN, Aksel'rod BM, Barchenko VT, Belousov VP, Egorova ZS, Igonchcnkov IV, Isakov AY, Kut'eva OY, Nikitin VA, Nikitin DV, Ruzaev SV, Rumyantsev AV, Tulyakov OS, Charykov NA, Yudovich ME, Yurin AL. Solution-solid phase equilibria in the fullerene $C_{60}$-fullerene $C_{70}$-$C_6H_5CH_3$ and fullerene $C_{60}$-fullerene $C_{70}$-*o*-$C_6H_4(CH_3)_2$ systems at 25 and 80°C, respectively. *Russ J Phys Chem*. 2000;74:1942–1945.
36. Odagiri T, Chan YC, Kwok KS, Ng KM. A novel evaporative crystallization column for the purification of fullerene $C_{60}$. *AIChE J*. 2007;53:531–534.

*Manuscript received May 3, 2009, and revision received Sep. 29, 2009.*